

Identification of a Calcium-Related Prognostic Signature and Validation of CACNA1B as a Driver of Metastasis in Hepatocellular Carcinoma

Yanling Chen^{1,*}, Yarong Ma^{1,*}, Guorui Zhao^{1,2,*}, Jianhao Li^{1,2}, Guizhen Zhang^{1,2}

¹Department of Infectious Diseases, The First Affiliated Hospital of Zhengzhou University, Zhengzhou, People's Republic of China; ²Gene Hospital of Henan Province, The First Affiliated Hospital of Zhengzhou University, Zhengzhou, People's Republic of China

*These authors contributed equally to this work

Correspondence: Guizhen Zhang, Department of Infectious Diseases, The First Affiliated Hospital of Zhengzhou University, No. 1 Jianshe East Road, Erqi District, Zhengzhou, Henan, 450052, People's Republic of China, Tel +8618337174928, Email zhgzmedicine@163.com

Purpose:: Hepatocellular carcinoma (HCC) is a significant global health burden. Cancer cells often exhibit an imbalance in intracellular calcium homeostasis. This study aims to explore the relationship between calcium-related genes and the prognosis of HCC, and establish a prognostic model based on calcium-related genes.

Methods: This study comprehensively reviewed 392 calcium-related regulators and constructed a Calcium-related Prognostic Risk Score (CPRS) for HCC by means of bootstrap-based univariate Cox, random forest screening, and LASSO analysis. We developed an effective prognostic nomogram for patients with HCC by integrating the CPRS and clinicopathological features. The signature was developed using the TCGA cohort and validated in two independent external cohorts (ICGC and NODE-CHCC). Subsequently, we identified the key genes in CPRS that affect the prognosis of HCC based on SurvSHAP, and further investigated the impact of the key factor CACNA1B on the biological behavior of HCC cells.

Results: CPRS was established with 6 calcium-related genes (CSN1S1, S100A9, CACNA1B, FKBP1A, SLC25A24 and SPP1). Our study showed that high CPRS is closely associated with higher histological grade, advanced TNM stage, vascular invasion, poorer progression-free and overall survival (OS) status of HCC, and CPRS can serve as an independent risk factor for the prognosis of HCC patients. The nomogram combining CPRS with TNM stage and patient age significantly improved the accuracy of predicting survival outcomes in HCC patients. Functional experiments revealed that inhibiting CACNA1B expression significantly suppressed cell proliferation, migration, and epithelial-mesenchymal transition signaling in HCC cells.

Conclusion: We developed a novel CPRS that can accurately predict the prognosis of HCC. CACNA1B may function as a tumor promoter in HCC progression.

Keywords: hepatocellular carcinoma, calcium-related gene, CACNA1B, risk score

Introduction

Hepatocellular carcinoma (HCC) ranks as the sixth most common malignancy and the third leading cause of cancer-related deaths worldwide.¹ Its incidence is rising rapidly, particularly in western countries, where non-alcoholic fatty liver disease and metabolic dysfunction-associated steatotic liver disease are emerging as dominant etiological factors, alongside traditional drivers such as chronic hepatitis B and C infections, and alcohol-related liver disease.² Over 60% of HCC cases are diagnosed outside surveillance, often via emergency presentations or late-stage symptomatic routes, correlating with poorer outcomes.³ Over the past decade, substantial efforts have been devoted to identifying gene signatures associated with the prognosis of HCC.⁴ However, the majority of these investigations have centered on developing prognostic models for overall survival (OS), placing minimal focus on the biological mechanisms underlying tumor progression, particularly invasion and metastasis, thereby restricting their value in guiding clinical decision-

making.⁵ Recently, research on specific biological processes such as methionine metabolism and autophagy has significantly improved the prognosis prediction of HCC and provided important insights into tumor progression and metastasis.^{6–9} These findings emphasize that process specific molecular signatures can capture not only survival risk but also the propensity for invasion and metastasis. Thus, it is imperative to develop HCC-specific prognostic biomarkers that are closely associated with metastatic behavior and to identify promising therapeutic targets based on the specific biological processes that drive tumor progression.

Calcium ions, serving as second messengers, participate in regulating various cellular activities such as proliferation, migration, and differentiation.¹⁰ Tumor cells commonly exhibit an imbalance in calcium homeostasis, characterized by abnormally elevated intracellular Ca^{2+} concentration, upregulation of calcium channels (such as TRPC6, ORAI1), and dysfunction of calcium pumps (such as SERCA), driving the malignant phenotype of tumors.¹¹ In the DMD gene deficient gastric cancer model, Ca^{2+} overload activates the calcium signaling pathway, leading to a decrease in mitochondrial membrane potential, while upregulation of glycolytic enzyme HK2/LDHA expression accelerates lactate secretion.¹² Mitochondria, as calcium storage reservoirs, have disrupted regulation of Ca^{2+} , which is directly associated with tumor drug resistance. Drug resistant cells often exhibit low intracellular Ca^{2+} concentration, leading to weakened endoplasmic reticulum stress and resistance to apoptosis.^{13,14} Clinical observations in several cancer types also suggest that elevated serum calcium levels or aberrant expression of calcium-associated molecules are frequently linked to high grades, advanced stages, lymph node metastasis, implying a pro-tumorigenic role of calcium in malignant progression.¹⁵ The liver, as a central metabolic organ, relies heavily on calcium signaling to regulate key physiological processes including glucose, lipid metabolism, and mitochondrial function.^{16,17} Disruption of calcium homeostasis in hepatocytes has been implicated in the pathogenesis of various liver diseases, including metabolic dysfunction-associated fatty liver disease (MAFLD) and its progression to HCC.^{18,19} However, despite increasing recognition of the importance of calcium signaling in tumors, the role of calcium related genes in HCC progression and prognosis remains largely unexplored. It is unclear whether specific calcium-related regulators can effectively stratify the risk of HCC patients and provide clues for personalized treatment.

In this study, we systematically characterized calcium-related genes in HCC and developed a calcium-related prognostic risk score (CPRS) (Figure 1). A total of 392 calcium related genes were screened for differential expression and survival analysis, and then feature selection was performed based on regression analysis to construct CPRS. The prognostic signature was comprehensively evaluated through survival analysis, assessment of clinicopathological correlations, and functional enrichment analysis. Furthermore, the CPRS was integrated with conventional clinicopathological parameters to generate a prognostic nomogram for HCC patients. Integrated bioinformatics analysis highlighted CACNA1B as a key component of the CPRS, and its expression was found to be markedly upregulated in metastatic HCC. Further experiments confirmed that silencing CACNA1B can inhibit the proliferation and metastasis of HCC cells, and it may participate in liver cancer cell metastasis by regulating the EMT pathway. Collectively, this study successfully constructed a novel and robust calcium-related prognostic model for HCC patients. And we validated that the key calcium regulatory factor CACNA1B can promote the malignant phenotype of HCC. The present study provides the rationale for more precise prognostic stratification of HCC patients and the development of novel therapeutics that target calcium metabolism regulators.

Materials and Methods

Datasets

Gene expression and Clinical data were collected from various public resources, such as The Cancer Genome Atlas (TCGA), the International Cancer Genome Consortium (ICGC), and The National Omics Data Encyclopedia (NODE). The CHCC (Chinese HBV-related HCC) cohort, comprising 159 HCC patients originally reported by Fan et al, was accessed through the National Omics Data Encyclopedia (NODE) database (Project ID: OEP000321).²⁰ In this manuscript, this dataset is referred to as the “CHCC cohort”. Patients with complete clinical follow-up information and available sequencing data were included in the study. HCC patients with incomplete follow-up information or duplicate sequencing samples were excluded. Patients with complete clinical follow-up information and available sequencing data

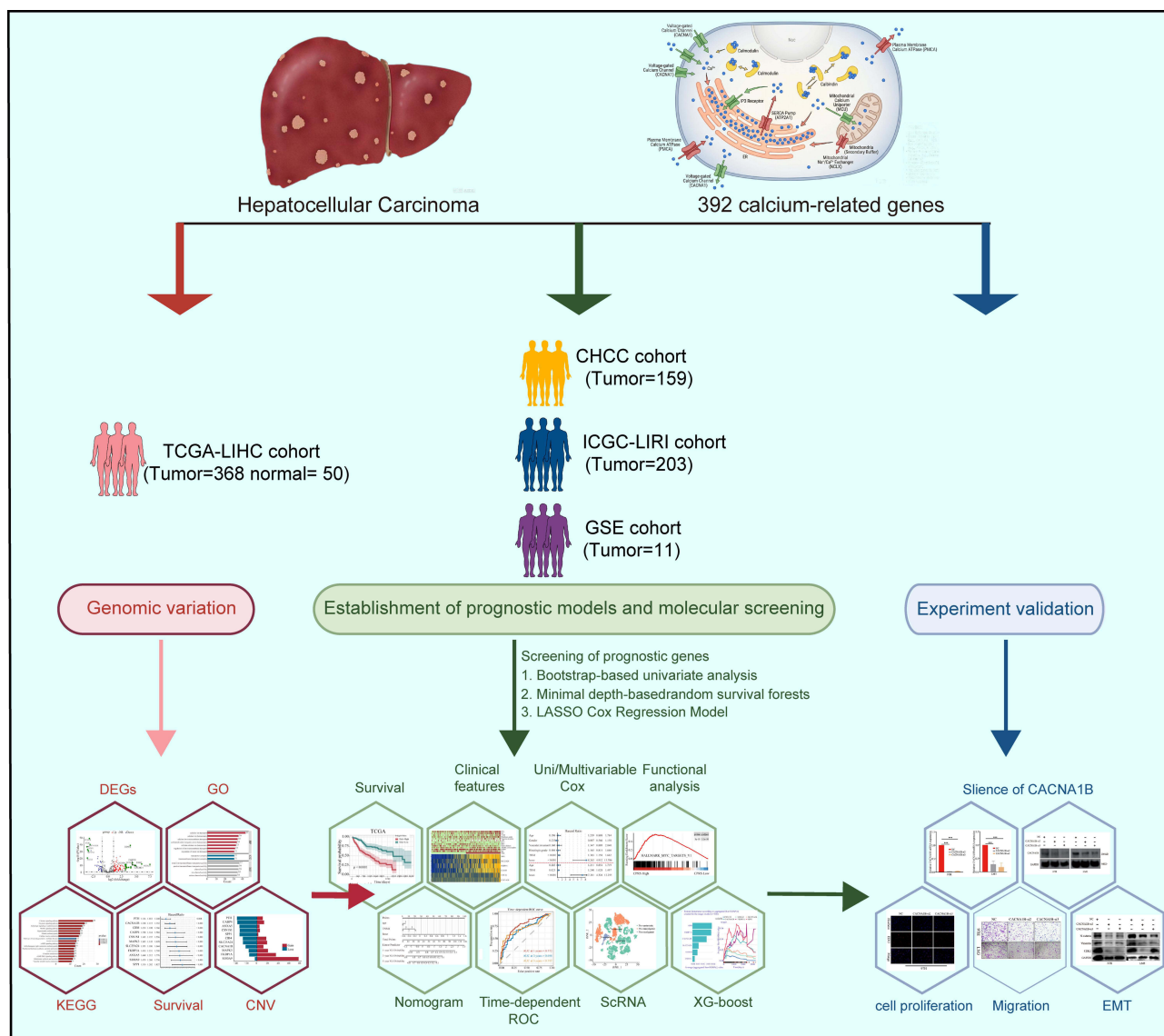


Figure 1 Flowchart for comprehensive analysis of calcium-related genes in HCC.

were included in the study. HCC patients with incomplete follow-up information or duplicate sequencing samples were excluded. To maintain consistency, The expression profiles were subjected to TPM normalization. The R package “maftools” was used to analyze somatic mutations. GSE149614 from the Gene Expression Omnibus database was used for single-cell sequencing (scRNA-seq) analysis of HCC. Additionally, annotations for cell subpopulations were acquired. The baseline clinical characteristics of the patients from each cohort have been summarized in [Supplementary Tables 1,2,8](#). Further information about cohorts is available in [Supplementary Table 3](#).

Identification and Validation of CPRS

The list of calcium-related genes was retrieved from the GeneCards database, and genes with a relevance score ≥ 8 were selected. The expression data of 392 calcium-related genes from the TCGA cohort were analyzed ([Supplementary Box 1](#)). During the screening procedure, 132 distinct differentially expressed genes (DEGs) were recognized. Subsequently, univariate Cox regression analysis was used to identify DEGs associated with overall survival (OS), which led to the identification of 11 significant DEGs. The dataset underwent 1000 rounds of bootstrapping, revealing that 85 DEGs showed a consistent association with prognosis across more than 900 iterations. In order to strengthen the

identification of genes related to prognosis, a Random Survival Forest method based on minimum depth was used to isolate 11 genes with the highest concordance index values from 1000 trials. To address collinearity, 6 genes were incorporated into the least absolute shrinkage and selection operator (LASSO) Cox regression model and selected for constructing CPRS. The CPRS was calculated using the following formula:

$$CPRS = \sum_{i=1}^n Coef_i * x_i$$

Here, Coef_i signifies the coefficient, while x_i indicates the mRNA expression level of six regulators. This formula was employed to determine the CPRS for each person in both the training (TCGA) and validation (ICGC, CHCC) groups. Based on this score, patients were then stratified into high-risk and low-risk groups using the median CPRS value of the training cohort as the cut-off point. This threshold was subsequently applied to the validation cohorts to ensure consistency. The predictive performance of the CPRS regarding prognosis in HCC patients was evaluated by computing the time-dependent AUC.

Functional Enrichment Analysis

We used the “clusterProfiler” package in R to identify the potential biological pathways associated with DEGs. Gene Set Variation Analysis (GSVA) and Gene Set Enrichment Analysis (GSEA) were utilized to delve deeper into the differing biological function of the high- and low-CPRS groups. For these analyses, we made use of the “h.all.v2022.1.Hs.symbols.gmt” database, supported by the R packages “GSVA” and “GSEABase”.

SurvSHAP

SHAP (Shapley Additive exPlanS) is a model interpretation framework proposed by Lundberg and Lee in 2017, aimed at explaining the predictive behavior of any machine learning model by calculating the contribution of each input feature to the model’s single prediction result (ie. SHAP value). This methodology, supported by the “SurvSHAP” package, improves the clarity and understanding of machine learning predictions by providing comprehensive and time sensitive analysis for survival regression deep learning models.²¹

Cell Culture

Human hepatocellular carcinoma cell lines (MHCC-97H,HCC-LM3) were kindly provided by Procell Life Science&Technology Co.,Ltd. (Wuhan, China) and maintained in State Key Laboratory of Antiviral Drugs. MHCC-97H,HCC-LM3 were cultured in DMEM (Vivacell,Shanghai,China) containing 10% fetal bovine serum (Vivacell, Shanghai,China). When the confluence reached 80%, the cells were employed for subsequent experiments.

siRNA Interference

siRNA sequences ([Supplementary Table 4](#)) were employed to achieve silencing of the CACNA1B gene. siRNA specifically targeting the CACNA1B, along with a negative control, was purchased from Obio Technology (Shanghai, China) Corp.,Ltd. The transfection was performed using jetPRIME[®] DNA/siRNA transfection reagent (Polyplus-transfection[®], France) following the manufacturer’s instructions.

Real-Time Quantitative PCR

RNA was extracted utilizing TRIzol[™] (Thermo Fisher Scientific, USA). Reverse transcription was carried out with the 1st Strand cDNA Synthesis Kit (Takara, Japan), followed by quantitative PCR using the SYBR Green Mix (Zoman Biotech, China). The primers produced by Songo Biotech (Shanghai, China) are detailed in [Supplementary Table 5](#). The target mRNA expression level was normalized against GAPDH.

Western Blot

Protein extraction was performed using RIPA containing PMSF to lyse cells (NCM Biotech,China). 20–30μg protein was loaded onto the gel (NCM Biotech,Suzhou,China) and then subjected to electrophoresis for separation. Following this,

the proteins were transferred onto PVDF membranes. Blocking was performed using 5% milk for 1 hour at room temperature. Primary antibodies were diluted in antibody diluent (Solarbio, China) and incubated overnight at 4°C. After washing, the PVDF membrane was incubated with secondary antibody, followed by detection using a chemiluminescence imaging system. The detailed information of antibodies is presented in [Supplementary Table 6](#).

CCK8 Assay

Cells were seeded onto 96-well plate. After the cells adhere to the plate wall, 10 μ L CCK-8 reagent (Solarbio, China) was added to incubate 1.5 hours. The optical density (OD) at 450 nm was detected with a microplate reader (Biotek, USA) at 0 hours, 24 hours, 48 hours, 72 hours, and 96 hours.

EdU Staining

Following a 48-hour transfection period, cells treated with CACNA1B siRNA and negative control were seeded onto 24-well plates and subjected to EdU staining. Subsequently, cells were fixed, permeabilized, and incubated with click additive solution. The nuclei were stained with Hoechst 33342. A fluorescence microscope (Olympus, Japan) was utilized to collect images. EdU staining was performed by EdU assay kit (Servebio, China).

Colony Formation

For this experiment, 1000 cells were seeded in each well of 6-well plates and cultured for 12–14 days. Following fixation with paraformaldehyde for 15 minutes, the colonies were stained with 0.1% crystal violet (Solarbio, China) for 10 minutes. Finally, the colonies were counted.

Transwell Assay

Transwell chamber (Corning, USA) were used for migration experiments. Place 200 μ L serum-free medium containing cells in the upper chamber, and add 600 μ L medium with 10% FBS in the lower chamber. After 24 hours incubation, soak both chambers in 10% formaldehyde and stain them with 0.1% crystal violet for 15 minutes. Then wipe the upper chamber with cotton swabs to remove cells. Finally, count the cells stained on the surface of the lower membrane under a microscope.

Statistical Analysis

Statistical analyses were performed by R version 4.0.4 and graphadprism. Differences between two groups were evaluated using a two-tailed, unpaired Student's *t*-test. The correlation between CPRS and clinical characteristics was determined by Chi-square tests. Kaplan-Meier survival analysis used the median CPRS, and the significance was evaluated by Log rank test. Univariate and multivariate Cox regression analyses determined the relationship between variables and outcomes. P value <0.05 was recognized as significant (* P < 0.05; ** P < 0.01, ***P < 0.0001).

Results

Landscape of Genetic Variation of Calcium-Related Genes in HCC

We first acquired the expression profile of 392 calcium-related genes from the TCGA-LIHC dataset. Differential expression analysis identified 132 significantly dysregulated genes (P and FDR < 0.05, $|\log_2FC| > 1$), including 98 upregulated and 34 downregulated genes in HCC tissues compared with normal liver tissues ([Figure 2A](#) and [B](#)). These differentially expressed calcium-related genes (DE-CaRGs) are summarized in [Supplementary Table 7](#). GO and KEGG enrichment analyses revealed that the DE-CaRGs were predominantly enriched in biological processes and molecular functions such as calcium ion transmembrane transport, regulation of cellular calcium ion homeostasis, cation channel activity, the cAMP signaling pathway, MAPK signaling, and multiple cardiovascular- and endocrine-related pathways ([Figure 2C](#) and [D](#)). To explore their prognostic relevance, we first performed univariate Cox regression with bootstrap resampling, identifying 11 calcium-related genes which were consistently and markedly associated with OS of HCC patients ([Figure 2E](#)). Copy number variation (CNV) analysis further demonstrated that several of these prognosis-

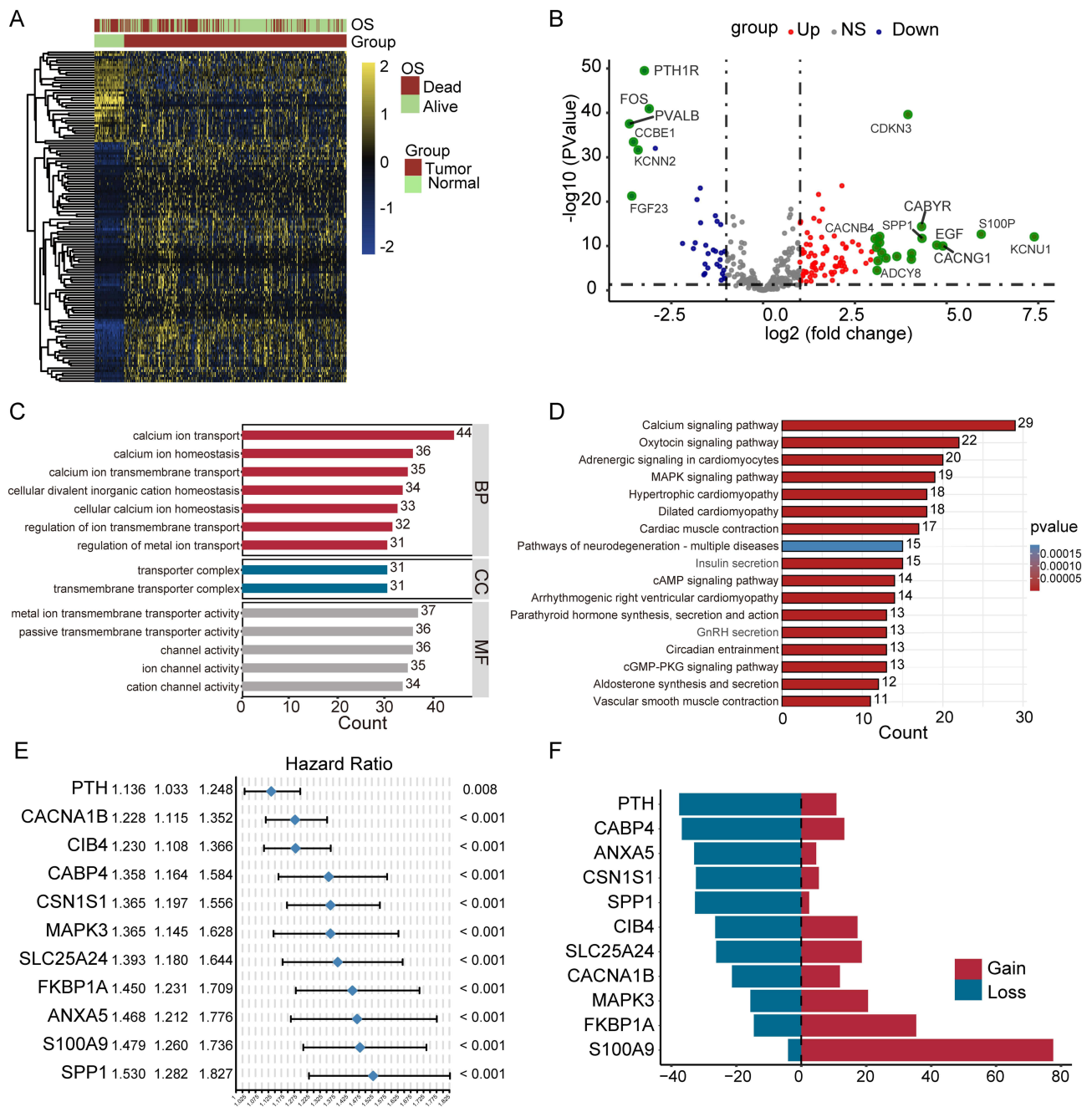


Figure 2 The expression profile and prognostic significance of calcium-related genes in HCC. **(A)** Heatmap of 392 calcium-related DEGs between HCC and normal tissues. **(B)** Volcano plot of DEGs. **(C and D)** GO enrichment **(C)** and KEGG **(D)** pathway analysis based on 392 DEGs. **(E)** Univariate Cox analysis of OS in HCC. **(F)** CNV values of calcium-related genes in the TCGA cohort.

Abbreviation: NS, Not Significant.

related genes exhibited frequent genomic alterations, with SPP1, S100A9, CACNA1B, FKBP1A, and SLC25A24 showing a predominance of copy number gains, whereas a smaller subset displayed copy number losses (Figure 2F). Collectively, these findings indicate that calcium-related genes are widely dysregulated at both the transcriptomic and genomic levels in HCC and may have important prognostic implications.

Construction of the CPRS and Its Clinical Characteristics

To identify the prognostic value of calcium-related genes in HCC, 11 OS-associated CaRGs obtained from the bootstrap-Cox and random forest screening were subjected to LASSO Cox regression. Using the minimum-lambda criterion, six hub genes—CSN1S1, S100A9, CACNA1B, FKBP1A, SLC25A24, and SPP1—were ultimately selected to construct the calcium-related prognostic risk score (CPRS) (Figure 3A and B). The CPRS for each patient was calculated as follows: $CPRS = \sum (\text{coefficient}_i \times \text{expression}_i \text{ of the six genes})$. HCC patients in the training cohort (TCGA) and the two external validation cohorts (ICGC and CHCC) were stratified into high- and low- CPRS groups according to the median CPRS. In all three cohorts, patients with high CPRS had worse OS than those with low CPRS, and risk score distribution and survival status plots showed an increased proportion of deaths with rising CPRS, accompanied by a clear expression gradient of the six genes between risk groups (Figure 3C–E).

To further elucidate the clinical relevance of the CPRS, we examined its association with key clinicopathological characteristics in the TCGA-LIHC cohort. Higher CPRS values were associated with higher histologic grade, advanced TNM stage, the presence of vascular invasion, and poorer progression free and OS status (Figure 4A and B;

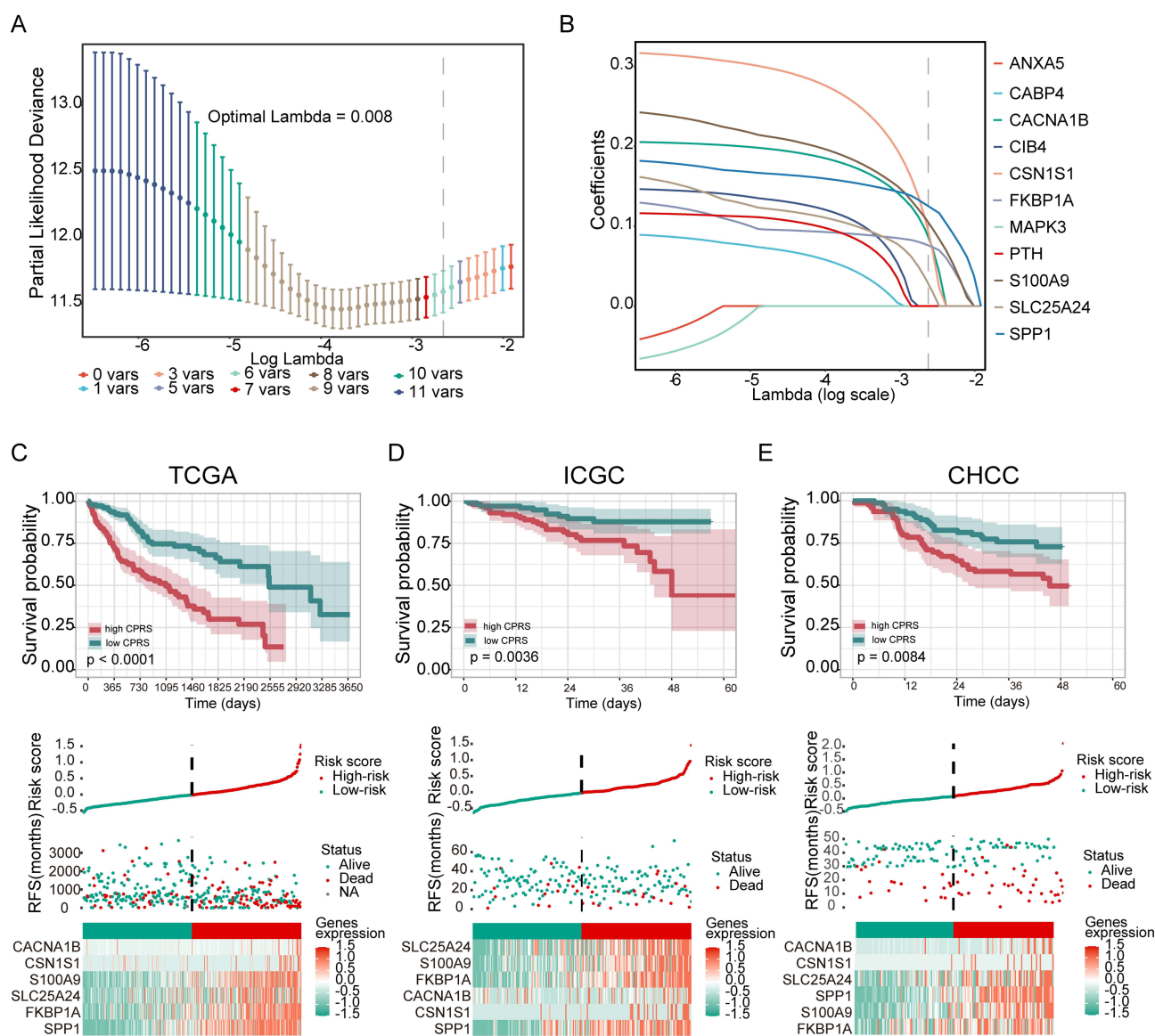


Figure 3 Construction and validation of the risk signature. (A and B) Model optimization and gene selection based on LASSO analysis (C–E) OS analyses for high-CPRS and low-CPRS groups in the training (C) cohort and validation (D and E) cohort.

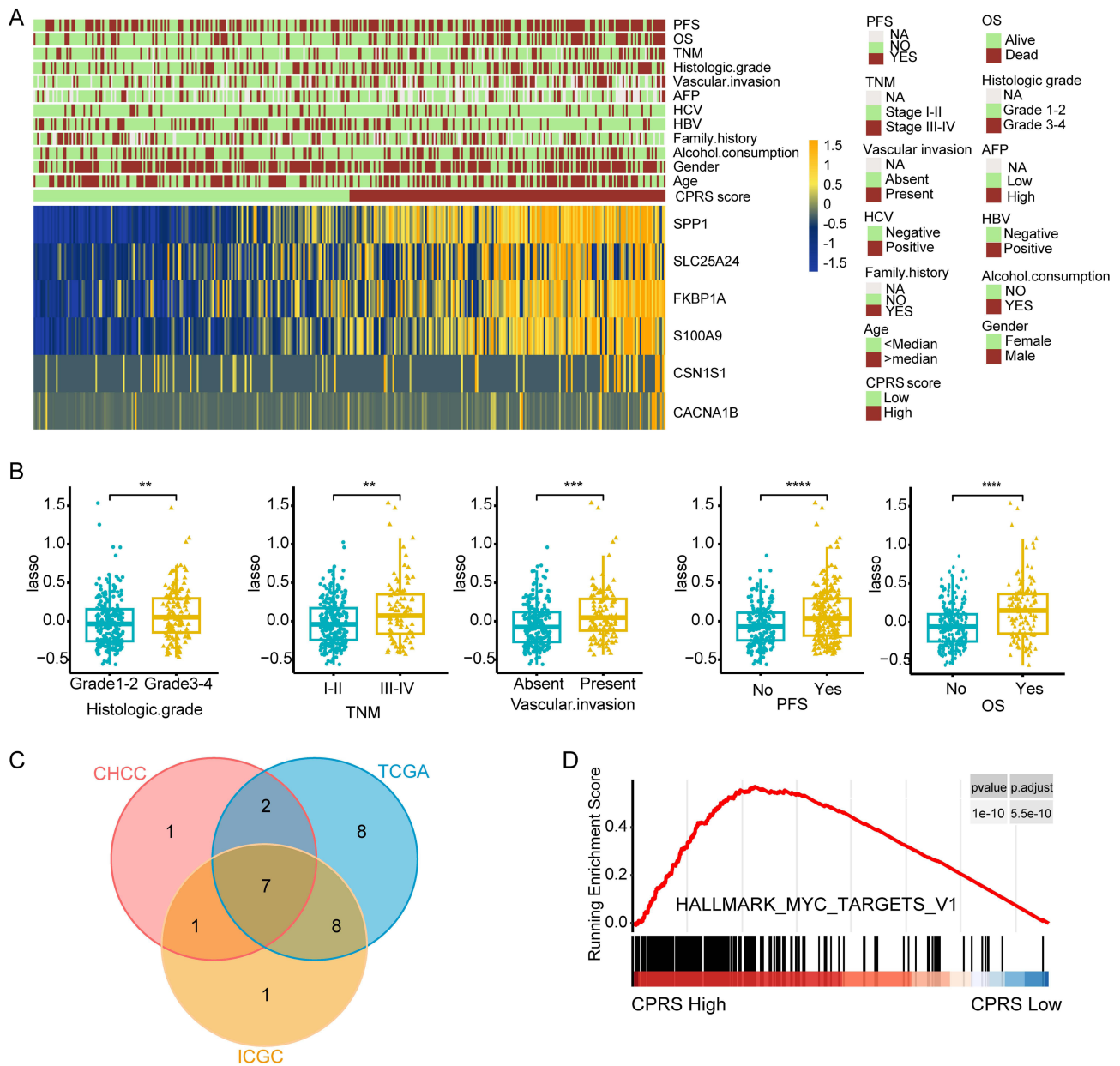


Figure 4 Clinical correlation and prognostic utility of the CPRS. **(A)** Clinicopathological features stratification by risk groups. **(B)** The relationships between the CPRS and clinical features. **(C)** A venn diagram from GSVA. **(D)** GSEA based on the TCGA-LIHC cohort. ** $P \leq 0.01$, *** $P \leq 0.001$, **** $P \leq 0.0001$. **Abbreviation:** NA, Not Available.

Supplementary Table 8). Subsequently, we conducted GSVA to compare biological processes between high- and low-CPRS groups in the TCGA, ICGC, and CHCC cohorts, revealing a set of commonly altered pathways across all three datasets (Figure 4C, Supplementary Figure 1, Supplementary Table 9). Subsequent validation using GSEA in the TCGA-LIHC cohort showed that high-CPRS tumors were enriched in hallmark pathways related to cell proliferation, including MYC targets (Figure 4D). These results suggest that the adverse prognosis associated with high CPRS may be linked to enhanced proliferative signaling pathways in HCC.

Construction and Evaluation of the Nomogram

The univariate and multivariate Cox regression analyses confirmed that both the CPRS and the TNM stage serve as independent prognostic indicators for OS in patients with HCC (Figure 5A). Based on the TCGA-LIHC cohort, we

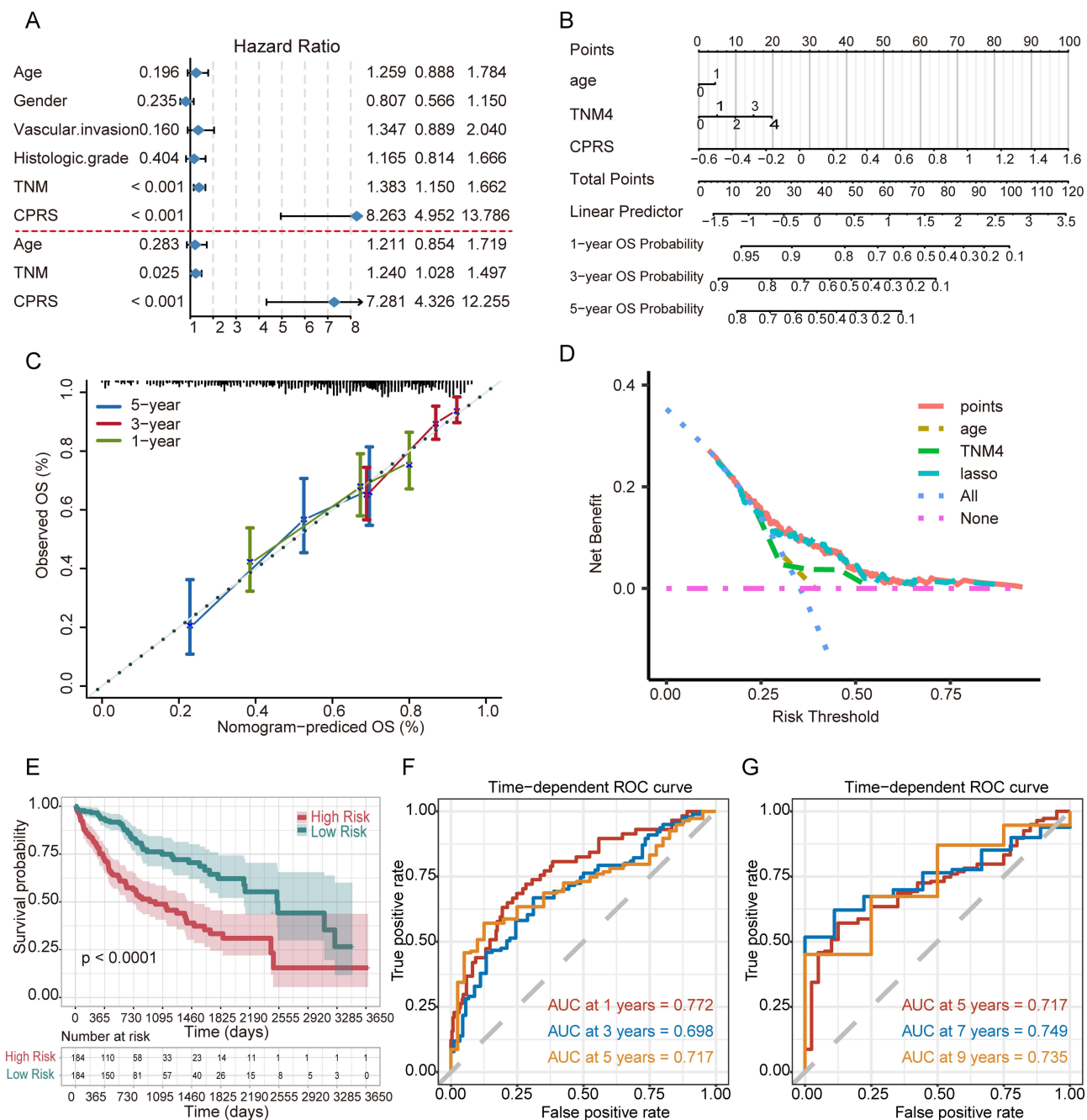


Figure 5 Establishment and evaluation of the nomogram survival model. (A) Univariate (up) and multivariate (down) Cox regression analyses based on TCGA-LIHC. (B) A nomogram was developed to estimate the prognosis for patients with HCC. (C) Model calibration analysis. (D) The decision curve analysis (DCA) assesses the nomogram's predictions for OS. (E) Survival probability stratification (Kaplan-Meier curves). (F and G) The OS prediction ability of nomogram was evaluated by ROC analysis.

constructed a prognostic nomogram integrating age, TNM stage, and CPRS to predict 1-, 3-, and 5-year OS (Figure 5B). Calibration curves indicated that the nomogram-predicted survival probabilities closely matched the observed outcomes at all three time points (Figure 5C). Decision curve analysis (DCA) indicated that the nomogram provided a greater net clinical benefit than individual clinical variables across a wide range of risk thresholds (Figure 5D). When patients were divided into high- and low-score groups according to the total nomogram score, the high-score group showed significantly poorer survival (Figure 5E). Time-dependent ROC analyses in TCGA-LIHC cohorts further confirmed the excellent discriminative ability of the nomogram, with robust AUC values for predicting 1-, 3-, 5-, 7-, and 9-year OS (Figure 5F and G). However, The model achieved AUC values of 0.674, 0.704, and 0.681 for 1-year, 3-year, and 5-year

PFS, respectively, indicating moderate predictive accuracy ([Supplementary Figure 2](#)). Overall, these findings indicate that CPRS-based nomogram is a reliable tool for individualized survival prediction in HCC patients.

Tumor Microenvironment Dissection Based on CPRS

Next, we analyzed scRNA-seq data from GSE149614 to investigate the distribution of CPRS at the single-cell level. Major cell populations, including hepatocytes, T cells, B cells, myeloid cells, endothelial cells, and fibroblasts, were annotated by canonical marker genes ([Figure 6A](#)). [Figure 6B](#) and [C](#) showed unique risk scoring patterns for different cell categories. Particularly, hepatocytes and myeloid cells exhibited significantly different levels of CPRS compared to other groups.

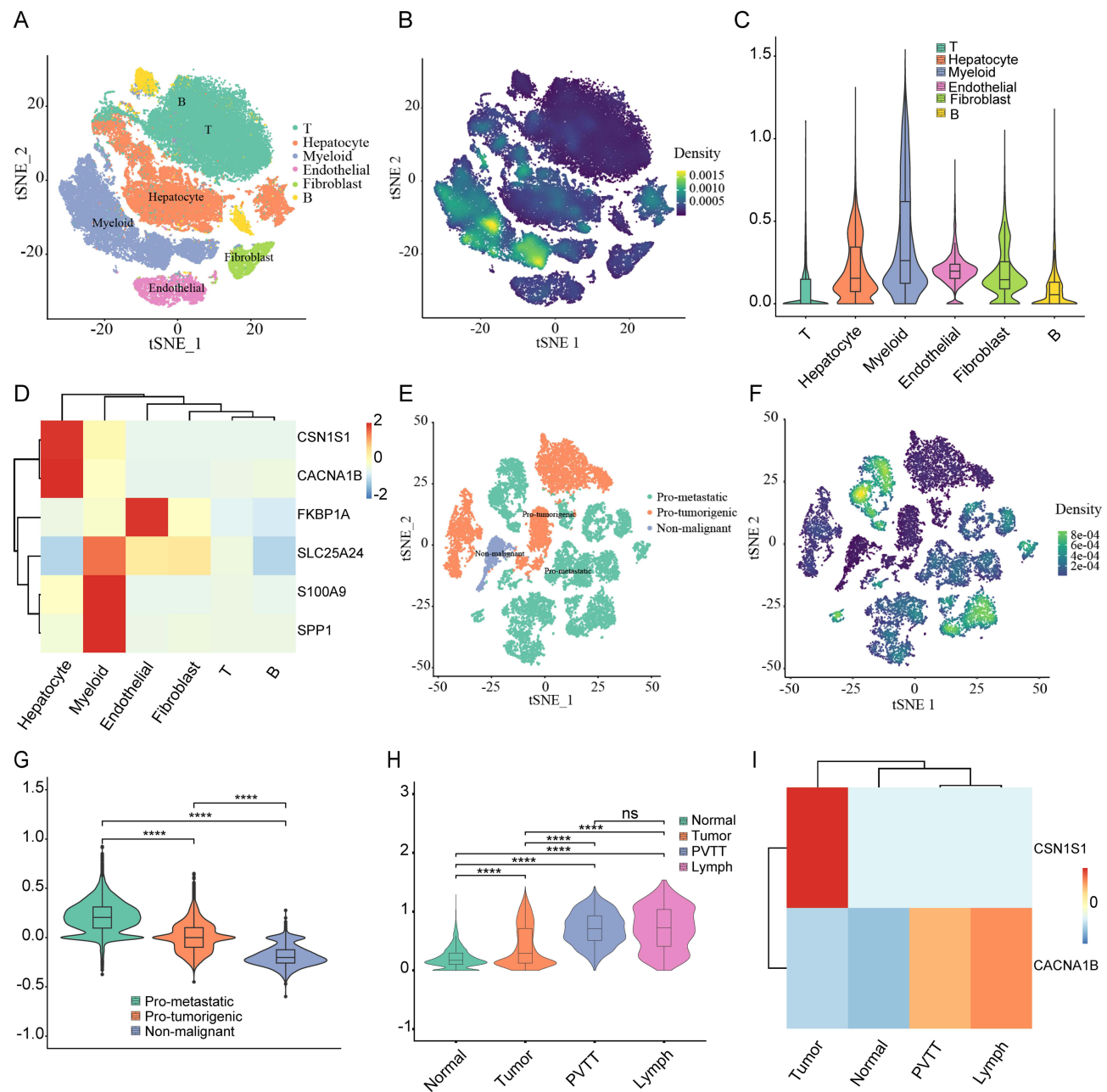


Figure 6 Single-cell transcriptomic profiling of calcium-related genes in HCC. **(A)** Single-cell clustering and cell type annotation using GSE149614 dataset. **(B–D)** Cell type-specific expression patterns of calcium-related genes in the tumor microenvironment. **(E)** t-SNE plot showing annotation of hepatocytes from HCC patients. **(F)** t-SNE plot showing CPRS density in hepatocyte subpopulations. **(G)** Violin plot of CPRS values for hepatocyte subpopulations. **(H)** Comparison of CPRS values between different liver cancer groups and the control group. **(I)** CACNA1B is highly expressed in metastatic liver cancer. **** $P \leq 0.0001$. **Abbreviation:** NS, Not Significant.

Further expression analysis also confirmed this result (Figure 6D). Considering the significant heterogeneity of hepatocytes, we classified them into pro-metastatic, pro-tumorigenic, and non-malignant subclusters based on transcriptional profiles (Figure 6E). The results demonstrated that compared with non-malignant cells, pro-metastatic hepatocytes and pro-tumorigenic cells have significantly increased CPRS values (Figure 6F and G). Subsequently, we compared the CPRS scores between portal vein metastasis (PVTT), lymph node metastasis, primary tumor, and adjacent non-tumor tissues, and found that the CPRS score of metastatic liver cancer was significantly higher than that of other groups (Figure 6H). In this study, we focused on the effect of calcium-related genes on cancer cells, and therefore conducted in-depth analysis of CSN1S1 and CACNA1B, which are highly expressed in HCC cells (Figure 6D). Figure 6I displayed that CACNA1B is predominantly overexpressed in metastatic tumors. These findings suggest that high CPRS is closely associated with the malignant state of hepatocytes and may be related to the metastasis potential of HCC cells.

Molecular Screening Based on SurvSHAP

To gain mechanistic insights into the CPRS and to prioritize key calcium-related regulators, we employed SurvSHAP. Using a random survival model based on CPRS, aggregated Shapley values were calculated to quantify the contribution of each gene to the predicted risk. The feature importance plot showed that SPP1, FKBP1A, CACNA1B, SLC25A24, S100A9, and CSN1S1 rank as the most influential variables, and SPP1 and FKBP1A exert the largest overall impact on survival prediction (Figure 7A). The SurvSHAP summary graph further illustrates how high expression levels of these genes are associated with increased risk, particularly SPP1, FKBP1A, and CACNA1B, whose elevated expression significantly shifts Shapley values towards worse outcomes (Figure 7B). These interpretability analyses highlight SPP1, FKBP1A, and CACNA1B as crucial elements of the CPRS. Previous studies have shown that SPP1 promotes liver cancer progression through various mechanisms such as resisting anoikis and reshaping the tumor immune microenvironment.^{22–24} FKBP1A plays a role as an “oncogene” in liver cancer, and its expression is upregulated in liver cancer tissues and cells. Knocking down FKBP1A can inhibit the proliferation and metastasis ability of liver cancer cells.²⁵ Nonetheless, the role of CACNA1B remains unclear. Thus, we examined how CACNA1B affects the behavior of HCC cells.

Silencing CACNA1B Suppresses HCC Progression

To validate the expression pattern of CACNA1B in HCC, RT-qPCR was performed on five pairs of HCC tissues and matched adjacent non-tumor tissues. As shown in Figure 8A, the mRNA level of CACNA1B was significantly higher in tumor tissues compared with adjacent normal tissues. To investigate the function of CACNA1B in HCC, siRNA was utilized to downregulate CACNA1B expression in HCC cell lines 97H and LM3. The knockdown efficiency was

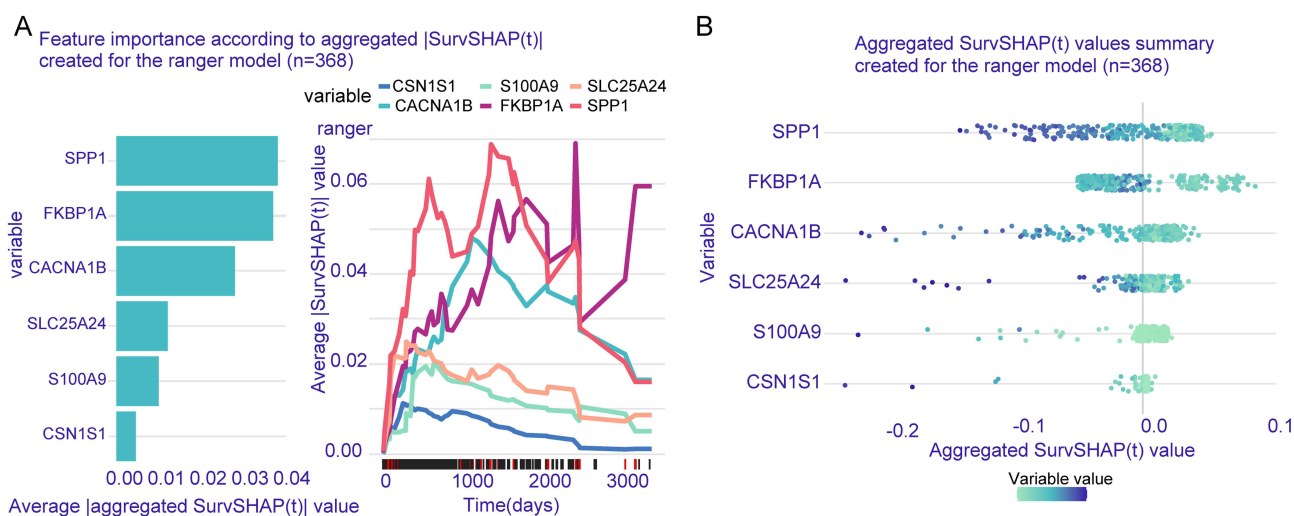


Figure 7 Model interpretation based on SurvSHAP. (A) SurvSHAP(t) values over time. (B) Six CPRS-related genes classified by SurvSHAP score.

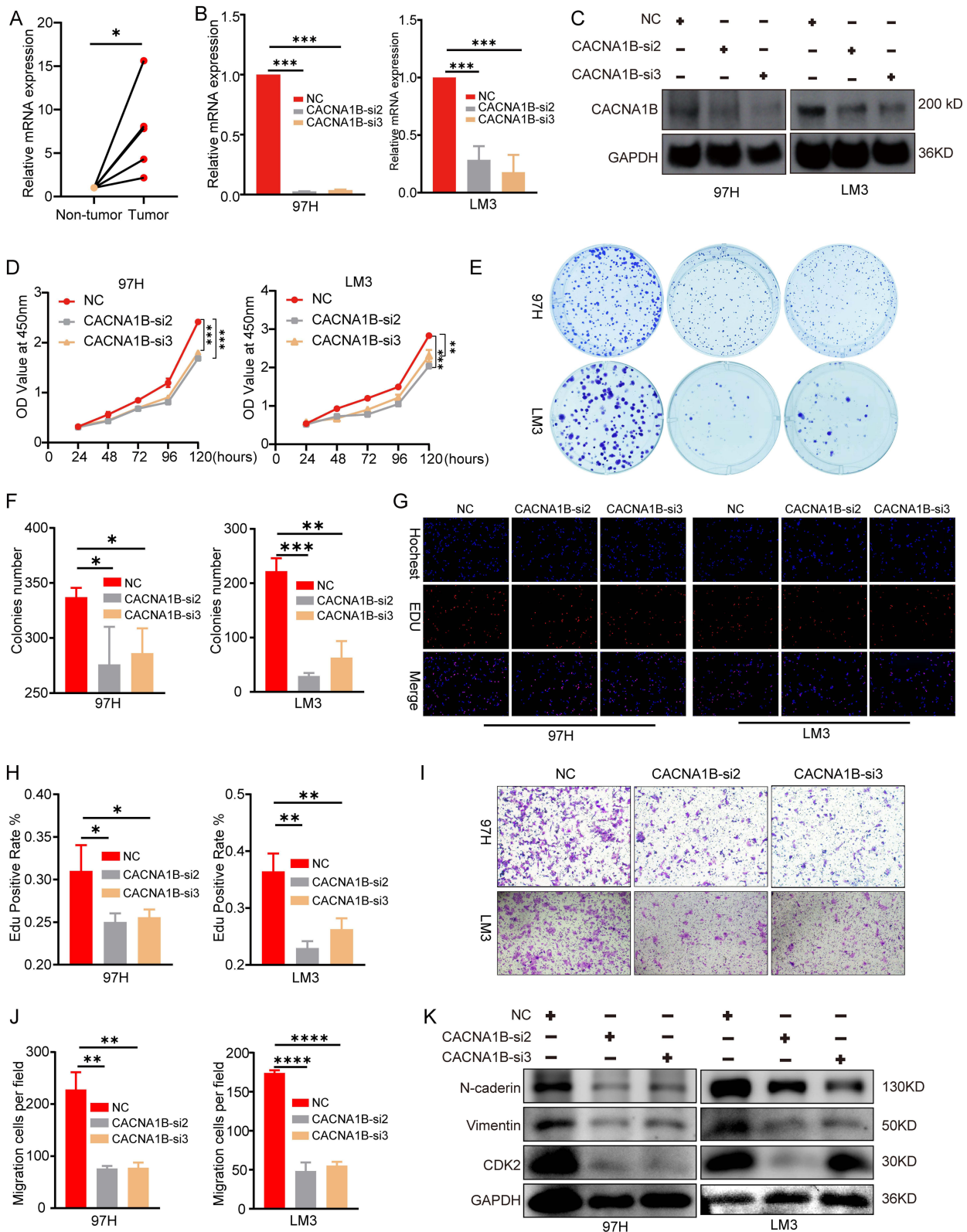


Figure 8 Silencing CACNA1B can inhibit the progression of HCC. **(A)** Relative mRNA expression of CACNA1B in HCC tissues and paired adjacent non-tumor tissues. Statistical analysis was performed using paired Student's *t*-test. **(B and C)** The siRNA-mediated silencing of CACNA1B was confirmed by RT-qPCR and immunoblotting. **(D–H)** CCK8 **(D)**, colony formation **(E and F)** and EdU **(G and H)** were implemented to assess cell proliferation ability. **(I and J)** The migration ability of cells was evaluated by a Transwell assay. **(K)** The relative expression of mesenchymal markers (N-cadherin, vimentin) and CDK2 after CACNA1B silencing. The unprocessed blots underlying **Figure 8** are provided in the Source Data of **Figure 8**. Data are presented as mean \pm SD from three independent experiments. Statistical comparisons between two groups were performed using Student's *t*-test (two-tailed, unpaired). **P* < 0.05, ***P* \leq 0.01, ****P* \leq 0.001, *****P* \leq 0.0001.

confirmed by RT-qPCR and Western blot (Figure 8B and C). The findings indicated that silencing of CACNA1B suppressed the proliferation (Figure 8D–H) and metastasis (Figure 8I and J) capacity of HCC cells.

To explore the potential mechanism by which CACNA1B promotes the progression of HCC, we performed Gene Set Variation Analysis (GSVA) comparing CACNA1B-high and CACNA1B-low groups across the TCGA, ICGC, and CHCC cohorts. As shown in [Supplementary Figure 3](#), the GSVA results revealed significant enrichment of oncogenic pathways in CACNA1B-high tumors, including cell cycle-related pathways (eg., G2-M checkpoint, E2F targets, mitotic spindle), epithelial-mesenchymal transition (EMT), apoptosis and key HCC driver pathways such as PI3K/AKT/mTOR and Notch signaling. Western blotting results showed that the expression of cell cycle promoting protein CDK2 and mesenchymal markers (N-cadherin, vimentin), were significantly decreased after knocking down CACNA1B (Figure 8K). These results are consistent with our bioinformatic predictions and provide experimental evidence that CACNA1B promotes HCC aggressiveness at least in part by modulating cell cycle progression and EMT.

Discussion

Hepatocellular carcinoma (HCC) remains one of the leading causes of cancer-related mortality worldwide, and its high recurrence and metastasis rates underscore the urgent need for robust prognostic biomarkers and novel therapeutic targets.¹ Calcium ions (Ca^{2+}) are classical second messengers that participate in various cellular processes, such as proliferation, migration, metabolism, and immune regulation.¹² Dysregulated calcium homeostasis has been implicated in the malignant transformation and progression of diverse tumor types through sustained remodeling of calcium flux and downstream signaling pathways.¹³ However, in HCC, a malignancy characterized by complex etiologies and pronounced intratumoral heterogeneity, systematic investigations into calcium-related genes and their prognostic significance have been limited. In particular, it remains unclear which calcium-related regulators integrate calcium signaling with metastatic behavior and clinical outcomes in HCC.

In this study, we comprehensively examined the expression and genomic landscape of 392 calcium-related genes in the TCGA-LIHC cohort and identified 132 differentially expressed calcium-related genes (DE-CaRGs), suggesting extensive disruption of the calcium signaling network in HCC. Functional enrichment analyses indicated that these DE-CaRGs are mainly involved in calcium ion transmembrane transport, regulation of cellular calcium ion homeostasis, cation channel activity, cAMP and MAPK signaling, as well as multiple cardiovascular- and endocrine-related pathways. These findings are consistent with the notion that aberrant activity of transmembrane calcium channels and transporters reprograms Ca^{2+} flux, thereby influencing key oncogenic pathways.¹³ Through bootstrap-Cox screening and random survival forest analysis, we narrowed down the gene list to 11 regulators closely related to OS, many of which exhibited frequent copy number alterations, further supporting their functional importance in HCC.

Using LASSO Cox regression, we ultimately identified a six-gene calcium-related signature and construct a CPRS. These genes play a regulatory role in calcium ion metabolism through different mechanisms, including extracellular matrix interaction (SPP1), inflammatory and immune modulation (S100A9), voltage-gated calcium influx (CACNA1B), calcium--dependent protein folding and signaling (FKBP1A), mitochondrial metabolite and ion transport (SLC25A24), and secreted calcium-binding proteins (CSN1S1). Patients with high CPRS had inferior OS and the risk score remained an independent prognostic factor after adjustment for conventional clinicopathological variables. Notably, high CPRS was strongly associated with advanced TNM stage, higher histologic grade, and vascular invasion, indicating that the CPRS can not only predict the survival of HCC patients, but also reflect the invasive clinical characteristics of liver cancer. Although sex has been reported to influence the prognosis of hepatocellular carcinoma (HCC),^{26,27} our analysis revealed no significant association between the CPRS and sex. This may be because the expression of the calcium-related genes comprising this signature is not substantially influenced by sex in our study cohort. Indeed, emerging evidence suggests that calcium-related molecules, such as the calcium-binding protein S100A1, can exhibit sex-specific regulatory roles in liver pathophysiology,²⁸ warranting further investigation into whether such mechanisms might affect the expression of CPRS components.

Mechanistically, our pathway analyses provide important clues as to how calcium dysregulation contributes to HCC progression. GSVA and GSEA consistently revealed that high-CPRS tumors are enriched in hallmark gene sets related to cell proliferation (MYC targets, E2F targets, G2M checkpoint) and metastasis (EMT). The dysregulation of these pathways has

been widely recognized in cancer progression. Thus, calcium-related genes may promote HCC progression by coordinating proliferative and survival programs, disrupting apoptotic control, and fostering a pro-invasive microenvironment.

Besides, we construct a prognostic nomogram that integrated CPRS, TNM stage, and age to further enhance clinical translation. This model achieved favorable calibration and discrimination for predicting 1-, 3-, and 5-year OS. Decision curve analysis demonstrated that the nomogram could provide greater net benefit than traditional clinicopathological factors. These results suggest that calcium-related regulators are prognostic biomarkers that can refine current risk stratification system for HCC, thereby facilitating individualized prognostic assessment and potentially guiding therapeutic decision-making.

Based on single-cell level analysis, the distribution of CPRS in the HCC tumor microenvironment was elucidated. CPRS values varied markedly across cell types, with the highest scores in hepatocytes and myeloid cells. When we divided hepatocytes into pro-metastatic, pro-tumorigenic, and non-malignant subclusters, results showed that pro-metastatic hepatocytes has the highest CPRS, and there is also a difference in scores between pro-tumorigenic cells and non-malignant cells. Several key CPRS genes, including SPP1, FKBP1A, CACNA1B, and SLC25A24, were preferentially expressed in the pro-metastatic subpopulation. These findings suggest that high CPRS is closely associated with the malignant state of liver cells and may at least partially reflect the metastatic potential of HCC cells. From a broader perspective, these results support that the dysregulation of calcium-related signaling may be a non-genetic heterogeneity that may affect the invasion, migration, and response to therapy of liver cancer.

CACNA1B encodes the $\alpha 1B$ subunit of N-type voltage-gated calcium channels, which are classically involved in neurotransmitter release but have increasingly been implicated in cancer progression.²¹ In our study, CACNA1B showed significant high expression in HCC tissues. This ectopic expression of a neuronal gene in liver cancer raises an intriguing biological question. Although CACNA1B is predominantly neuronal, its upregulation in non-neural tumors is not unprecedented. Several mechanisms may explain this phenomenon, including neuroendocrine transdifferentiation,²⁹ transcriptional dysregulation (eg., activation of neuronal transcription factors),^{30,31} and epigenetic reprogramming during hepatocarcinogenesis.³² The observed correlation between copy number gain and high expression suggests that genomic amplification may partially contribute. Future studies investigating the transcriptional and epigenetic regulation of CACNA1B in HCC would help elucidate why this neuronal channel is co-opted during liver tumorigenesis. SurvSHAP-based model interpretation confirmed that CACNA1B is one of the most influential determinants of the CPRS, with elevated expression contributing strongly to increased predicted risk. Functional experiments further demonstrated that silence of CACNA1B suppressed the proliferative and migratory abilities of HCC cells, supporting a direct oncogenic role.

Mechanistically, CACNA1B may accelerate cell cycle progression and participate in EMT transformation to promote the proliferation and metastasis of liver cancer. These data suggest that aberrant activation of N-type calcium channels may enhance Ca^{2+} influx, thereby sustaining oncogenic signaling and promoting HCC growth and metastasis. Given that CACNA1B has been explored as a druggable target in neurological disorders,^{33,34} these findings raise the intriguing possibility that pharmacological modulation of CACNA1B or N-type calcium channels could be repurposed or optimized for HCC treatment, particularly in patients with high CPRS. However, the clinical translation of this concept faces substantial challenges. Ziconotide, a selective Cav2.2 blocker approved for severe chronic pain, requires intrathecal administration due to its poor blood–brain barrier permeability, which limits its systemic bioavailability and makes it impractical for treating solid tumors such as HCC.³⁵ Moreover, the widespread expression of CACNA1B in the nervous system raises concerns about potential neurotoxicity or off-target effects upon systemic inhibition.³⁶ Therefore, direct repurposing of existing neurological drugs for HCC may not be feasible without significant modification. Future efforts could focus on developing novel small-molecule inhibitors with improved pharmacokinetic profiles and tumor selectivity, or exploring targeted delivery systems to minimize neurological adverse effects. Alternatively, screening FDA-approved calcium channel blockers with different selectivity profiles might identify existing drugs with unexpected anti-tumor activity and more favorable safety profiles for systemic use. Our findings provide a rationale for such investigations and highlight CACNA1B as a potential therapeutic vulnerability in HCC.

Other components of the CPRS also appear to participate in pro-tumorigenic calcium-dependent processes. SPP1 (osteopontin) is a secreted phosphoprotein that binds integrins and CD44, modulates calcium deposition, and has been repeatedly linked to HCC invasion, metastasis, and poor prognosis.³⁷ S100A9 is a calcium-binding protein involved in

inflammatory signaling and myeloid-derived suppressor cell function.^{38,39} Correlation between myeloid-derived suppressor cells and S100A8/A9 in tumor and autoimmune diseases.^{38,39} Its overexpression can foster a protumorigenic inflammatory microenvironment.^{40,41} FKBP1A participates in calcium-dependent regulation of TGF- β and mTOR signaling,^{42,43} while SLC25A24, a mitochondrial carrier protein, contributes to calcium buffering and energy metabolism, which may support rapid tumor growth under metabolic stress.⁴⁴ CSN1S1, although traditionally viewed as a milk protein, has emerging roles in modulating immune responses and calcium binding.⁴⁵ The convergent integration of these channels, transporters, and calcium-binding proteins into a single prognostic model underscores the centrality of calcium signaling in orchestrating multiple malignant hallmarks of HCC.

Our study also provides a framework for linking calcium-related prognostic signatures to potential therapeutic strategies. While we did not focus on specific calcium channel blockers or targeted agents in this work, previous clinical and preclinical studies have shown that pharmacological inhibition of certain calcium channels can exert anti-tumor effects in several cancer types.²¹ The strong association between high CPRS and aggressive, proliferation-driven, metastatic phenotypes suggests that combination regimens targeting both calcium channels (eg., CACNA1B or related components) and canonical oncogenic pathways may yield synergistic efficacy. Furthermore, given that CPRS is quantifiable at the transcriptomic level, it may serve as a biomarker for screening patients who could benefit from therapies targeting calcium metabolism, thereby optimizing personalized treatment.

Several limitations of our study should be acknowledged. First, although the CPRS was constructed and validated in multiple independent cohorts and demonstrated robust predictive performance, all primary analyses were retrospective and based on public datasets. Prospective validation in large, multi-center clinical cohorts is required before the CPRS can be routinely implemented in clinical practice. Second, the validation mainly focused on CACNA1B, however, the mechanisms through which other CPRS genes including FKBP1A, SLC25A24, and CSN1S1 drive HCC progression still need to be elucidated. Third, although single-cell analysis provided insights into the distribution of CPRS in the tumor microenvironment, functional experiments at the single-cell or spatial level are needed to confirm the relationship between calcium-related gene, cell subpopulations, and metastasis behavior. Finally, while our *in vitro* findings consistently support the protumorigenic role of CACNA1B in HCC, we acknowledge that direct measurement of calcium flux and *in vivo* animal studies would provide more definitive evidence for its mechanism and therapeutic potential. Future investigations incorporating calcium imaging and orthotopic tumor models are warranted to further validate our conclusions.

Conclusion

In this study, we systematically characterized the dysregulation of calcium-related genes in HCC and established a six-gene CPRS that could robustly predict survival and correlates with aggressive clinicopathological features. The CPRS-based nomogram provides a valuable tool for individualized risk stratification. Moreover, single-cell and model-interpretation analyses highlight CACNA1B together with SPP1, FKBP1A, SLC25A24, S100A9, and CSN1S1, as critical calcium-related regulators of HCC progression. These findings not only deepen our understanding of how aberrant calcium signaling shapes the malignant phenotype of HCC but also provide a rationale for further mechanistic and therapeutic exploration of CACNA1B and other calcium-related targets in this deadly disease.

Ethics Approval

The study protocol was approved by the Clinical Trial Ethics Committee of The First Affiliated Hospital of Zhengzhou University (approval number: 2025-KY-0870-002).

Acknowledgments

The authors thank citexs (<https://www.citexs.com>) for English language editing.

Funding

This work was supported by the Postdoctoral Fellowship Program of China Postdoctoral Science Foundation (NO. GZC20232430, NO.2024M752960), the Youth Project of Henan Natural Science Foundation (NO.252300420549).

Disclosure

The authors report no conflicts of interest in this work.

References

1. Bray F, Laversanne M, Sung H, et al. Global cancer statistics 2022: GLOBOCAN estimates of incidence and mortality worldwide for 36 cancers in 185 countries. *CA Cancer J Clin.* 2024;74(3):229–263. doi:10.3322/caac.21834
2. Kim DY. Changing etiology and epidemiology of hepatocellular carcinoma: asia and worldwide. *J Liver Cancer.* 2024;24(1):62–70. doi:10.17998/jlc.2024.03.13
3. Moris D, Martinino A, Schiltz S, et al. Advances in the treatment of hepatocellular carcinoma: an overview of the current and evolving therapeutic landscape for clinicians. *CA Cancer J Clin.* 2025;75(6):498–527. doi:10.3322/caac.70018
4. Rebouissou S, Nault JC. Advances in molecular classification and precision oncology in hepatocellular carcinoma. *J Hepatol.* 2020;72(2):215–229. doi:10.1016/j.jhep.2019.08.017
5. Flynn MJ, Sayed AA, Sharma R, Siddique A, Pinato DJ. Challenges and opportunities in the clinical development of immune checkpoint inhibitors for hepatocellular carcinoma. *Hepatology.* 2019;69(5):2258–2270. doi:10.1002/hep.30337
6. Sanderson SM, Gao X, Dai Z, Locasale JW. Methionine metabolism in health and cancer: a nexus of diet and precision medicine. *Nat Rev Cancer.* 2019;19(11):625–637. doi:10.1038/s41568-019-0187-8
7. Zheng Z, Xu H, Luo L. Autophagy-related gene SQSTM1 predicts the prognosis of hepatocellular carcinoma. *Comput Biol Med.* 2025;192:110358. doi:10.1016/j.combiomed.2025.110358
8. Wang J, Xie Q, Wu L, et al. Stromal interaction molecule 1/microtubule-associated protein 1A/1B-light chain 3B complex induces metastasis of hepatocellular carcinoma by promoting autophagy. *MedComm.* 2024;5(2):e482. doi:10.1002/mco.2482
9. Lu J, Ding Y, Zhang W, et al. SQSTM1/p62 knockout by using the CRISPR/Cas9 system inhibits migration and invasion of hepatocellular carcinoma. *Cells.* 2023;12(9):1238. doi:10.3390/cells12091238
10. Berridge MJ, Bootman MD, Roderick HL. Calcium signalling: dynamics, homeostasis and remodelling. *Nat Rev Mol Cell Biol.* 2003;4(7):517–529. doi:10.1038/nrm1155
11. Qin Z, Di Y, Ma T, Zeng W, Liu X, He W. The calcium homeostasis in tumor and the mechanism involving progression and metastasis. *Cancer Lett.* 2025;630:217908. doi:10.1016/j.canlet.2025.217908
12. Zou X, Wu T, Su T, et al. Disruption of DMD gene leads to altered calcium homeostasis and metabolic shift impacting gastric Cancer cell proliferation and migration. *Cancer Cell Int.* 2025;25(1):202. doi:10.1186/s12935-025-03829-4
13. Garbincius JF, Elrod JW. Mitochondrial calcium exchange in physiology and disease. *Physiol Rev.* 2022;102(2):893–992. doi:10.1152/physrev.00041.2020
14. Zhang L, Sun Y, Lin Y, et al. Cell calcification reverses the chemoresistance of cancer cells via the conversion of glycolipid metabolism. *Biomaterials.* 2025;314:122886. doi:10.1016/j.biomaterials.2024.122886
15. Roberts-Thomson SJ, Chalmers SB, Monteith GR. The calcium-signaling toolkit in cancer: remodeling and targeting. *Cold Spring Harb Perspect Biol.* 2019;11(8):a035204. doi:10.1101/cshperspect.a035204
16. Humbert A, Lefebvre R, Nawrot M, Caussy C, Rieusset J. Calcium signalling in hepatic metabolism: health and diseases. *Cell Calcium.* 2023;114:102780. doi:10.1016/j.ceca.2023.102780
17. Eberhardt DR, Chaudhuri D. Mitochondrial calcium signaling in hepatocyte health and disease. *Cold Spring Harb Perspect Biol.* 2025;a041773. doi:10.1101/cshperspect.a041773
18. Ali ES, Rychkov GY, Barritt GJ. Deranged hepatocyte intracellular Ca²⁺ homeostasis and the progression of non-alcoholic fatty liver disease to hepatocellular carcinoma. *Cell Calcium.* 2019;82:102057. doi:10.1016/j.ceca.2019.102057
19. Chen CC, Hsu LW, Chen KD, Chiu KW, Chen CL, Huang KT. Emerging roles of calcium signaling in the development of non-alcoholic fatty liver disease. *Int J Mol Sci.* 2021;23(1):256. doi:10.3390/ijms23010256
20. Gao Q, Zhu H, Dong L, et al. Integrated proteogenomic characterization of HBV-Related hepatocellular carcinoma. *Cell.* 2019;179(2):561–577. doi:10.1016/j.cell.2019.08.052
21. Cui C, Merritt R, Fu L, Pan Z. Targeting calcium signaling in cancer therapy. *Acta Pharm Sin B.* 2017;7(1):3–17. doi:10.1016/j.apsb.2016.11.001
22. Wang Y, Wang Q, Tao S, et al. Identification of SPP1+ macrophages in promoting cancer stemness via vitronectin and CCL15 signals crosstalk in liver cancer. *Cancer Lett.* 2024;604:217199. doi:10.1016/j.canlet.2024.217199
23. Zhang Z, Chen X, Li Y, et al. The resistance to anoikis, mediated by Sp1, and the evasion of immune surveillance facilitate the invasion and metastasis of hepatocellular carcinoma. *Apoptosis Int J Program Cell Death.* 2024;29(9–10):1564–1583. doi:10.1007/s10495-024-01994-x
24. Fan G, Xie T, Li L, Tang L, Han X, Shi Y. Single-cell and spatial analyses revealed the co-location of cancer stem cells and SPP1+ macrophage in hypoxic region that determines the poor prognosis in hepatocellular carcinoma. *NPJ Precis Oncol.* 2024;8(1):75. doi:10.1038/s41698-024-00564-3
25. Li Z, Cui Y, Duan Q, et al. The prognostic significance of FKBP1A and its related immune infiltration in liver hepatocellular carcinoma. *Int J Mol Sci.* 2022;23(21):12797. doi:10.3390/ijms232112797
26. Tran TT, Be HT, Hoang KD, Dong HD. Sex and gender disparities in hepatocellular carcinoma: insights into risk, diagnosis, and therapeutic outcomes. *Clin Transl Oncol.* 2025;27(12):4301–4315. doi:10.1007/s12094-025-03965-3
27. Chen J, Yang Z, Gao F, et al. Influence of sex on outcomes of liver transplantation for hepatocellular carcinoma: a multicenter cohort study in China. *Cancer Biol Med.* 2024;21(4):347–362. doi:10.20892/j.issn.2095-3941.2023.0453
28. Zhu M, Li Y, Shen Q, Gong Z, Liu D. Sex hormone receptors, calcium-binding protein and Yap1 signaling regulate sex-dependent liver cell proliferation following partial hepatectomy. *Dis Model Mech.* 2024;17(10):dmm050900. doi:10.1242/dmm.050900
29. Shi C, Jug R, Bean SM, Jeck WR, Guy CD. Primary hepatic neoplasms arising in cirrhotic livers can have a variable spectrum of neuroendocrine differentiation. *Hum Pathol.* 2021;116:63–72. doi:10.1016/j.humpath.2021.07.007
30. Wu Z, Duan W, Xiong Y, et al. NeuroD1 drives a KAT2A-FDFT1 signaling axis to promote cholesterol biosynthesis and hepatocellular carcinoma progression via histone H3K27 acetylation. *Oncogene.* 2025;44(42):4017–4031. doi:10.1038/s41388-025-03534-6

31. Gao Q, Wang K, Chen K, et al. HBx protein-mediated ATOH1 downregulation suppresses ARID2 expression and promotes hepatocellular carcinoma. *Cancer Sci.* 2017;108(7):1328–1337. doi:10.1111/cas.13277
32. Suvà ML, Riggi N, Bernstein BE. Epigenetic reprogramming in cancer. *Science.* 2013;339(6127):1567–1570. doi:10.1126/science.1230184
33. Tang C, Gomez K, Chen Y, et al. C2230, a preferential use- and state-dependent CaV2.2 channel blocker, mitigates pain behaviors across multiple pain models. *J Clin Invest.* 2024;135(4):e177429. doi:10.1172/JCI177429
34. Manda P, Kushwaha AS, Kundu S, Shivakumar HN, Jo SB, Murthy SN. Delivery of ziconotide to cerebrospinal fluid via intranasal pathway for the treatment of chronic pain. *J Control Release off J Control Release Soc.* 2016;224:69–76. doi:10.1016/j.jconrel.2015.12.044
35. Pope JE, Deer TR. Ziconotide: a clinical update and pharmacologic review. *Expert Opin Pharmacother.* 2013;14(7):957–966. doi:10.1517/14656566.2013.784269
36. Schmidtko A, Lötsch J, Freynhagen R, Geisslinger G. Ziconotide for treatment of severe chronic pain. *Lancet.* 2010;375(9725):1569–1577. doi:10.1016/S0140-6736(10)60354-6
37. Wang K, Wan J, Zheng R, et al. SPP1 as a prognostic and immunotherapeutic biomarker in gliomas and other cancer types: a pan-cancer study. *J Inflamm Res.* 2025;18:2247–2265. doi:10.2147/JIR.S505237
38. Razmkhah F, Kim S, Lim S, Dania AJ, Choi J. S100A8 and S100A9 in hematologic malignancies: from development to therapy. *Int J Mol Sci.* 2023;24(17):13382. doi:10.3390/ijms241713382
39. Zheng R, Chen S, Chen S. Correlation between myeloid-derived suppressor cells and S100A8/A9 in tumor and autoimmune diseases. *Int Immunopharmacol.* 2015;29(2):919–925. doi:10.1016/j.intimp.2015.10.014
40. De Veirman K, Van Valckenborgh E, De Beule N, et al. Targeting S100A9 interactions in the multiple myeloma bone marrow environment reduces angiogenesis and tumor growth. *Blood.* 2016;128(22):3248. doi:10.1182/blood.V128.22.3248.3248
41. Luo W, Su X, Zhang Q, et al. S100A8/A9 perturbation in bone marrow blunts antitumor immunity by promoting protumorigenic myelopoiesis in mouse models. *Sci Transl Med.* 2025;17(807):eadr3963. doi:10.1126/scitranslmed.adr3963
42. Chen W, Que Q, Zhong R, Lin Z, Yi Q, Wang Q. Assessing TGF- β prognostic model predictions for chemotherapy response and oncogenic role of FKBP1A in liver cancer. *Curr Pharm Des.* 2024;30(39):3131–3152. doi:10.2174/0113816128326151240820105525
43. Ge D, Han L, Huang S, et al. Identification of a novel mTOR activator and discovery of a competing endogenous RNA regulating autophagy in vascular endothelial cells. *Autophagy.* 2014;10(6):957–971. doi:10.4161/auto.28363
44. Gao Y, Peng Y, Zhou Y, et al. Mitochondrial gene SLC25A24 regulated anti-tumor immunity and inhibited the proliferation and metastasis of colorectal cancer by PKG1-dependent cGMP/PKG1 pathway. *Int Immunopharmacol.* 2025;157:114664. doi:10.1016/j.intimp.2025.114664
45. Vordenbäumen S, Braukmann A, Altendorfer I, Bleck E, Jose J, Schneider M. Human casein alpha s1 (CSN1S1) skews in vitro differentiation of monocytes towards macrophages. *BMC Immunol.* 2013;14:46. doi:10.1186/1471-2172-14-46

Journal of Hepatocellular Carcinoma

Publish your work in this journal

The Journal of Hepatocellular Carcinoma is an international, peer-reviewed, open access journal that offers a platform for the dissemination and study of clinical, translational and basic research findings in this rapidly developing field. Development in areas including, but not limited to, epidemiology, vaccination, hepatitis therapy, pathology and molecular tumor classification and prognostication are all considered for publication. The manuscript management system is completely online and includes a very quick and fair peer-review system, which is all easy to use. Visit <http://www.dovepress.com/testimonials.php> to read real quotes from published authors.

Submit your manuscript here: <https://www.dovepress.com/journal-of-hepatocellular-carcinoma-journal>

Dovepress
Taylor & Francis Group